Adriaan J. Teuling and Peter A. Troch (2004), **Simulating soil moisture variability dynamics**, in *Proceedings of the 2nd international CAHMDA workshop on: The Terrestrial Water Cycle: Modelling and Data Assimilation Across Catchment Scales*, edited by A.J. Teuling, H. Leijnse, P.A. Troch, J. Sheffield and E.F. Wood, pp. 81–85, Princeton, NJ, October 25–27

Simulating soil moisture variability dynamics

Adriaan J. Teuling[1] **and Peter A. Troch**[1]

[1]*Hydrology and Quantitative Water Management Group, Wageningen University, Wageningen, The Netherlands*

During previous field experiments, different trends of soil moisture variability with mean moisture content have been reported. Here we explain these trends for three different data sets by showing how the different controls interact to either create or destroy spatial variance. Improved understanding of these processes is needed for the transformation of point-scale measurements and parameterizations to scales required for climate studies, operational weather forecasting, and large scale hydrological modeling.

Introduction Although the quantitative contribution of soil moisture to the global water budget is negligible, it plays a central role in the global water cycle by controlling the partitioning of water and energy fluxes at the earth's surface, and may control the continental water distribution through land-surface atmosphere feedback mechanisms (*Koster et al.*, 2003). The ability of coupled models to reproduce these processes will strongly depend on the parameterization of soil moisture state-flux relationships at the regional scale. The lack of accurate observations of land surface states and fluxes at the regional scale, combined with the variability of soil moisture and the high non-linearity of land-surface processes at the small scale, requires aggregation of small scale processes to larger scales in order to prevent systematic biases in modeled water- and energy fluxes (*Crow and Wood*, 2002). For successful aggregation, knowledge on soil moisture variability controls is indispensible.

Several scientists have reported soil moisture variability to increase with decreasing mean moisture content (e.g. *Famiglietti et al.*, 1999; *Hupet and Vanclooster*, 2002). Other scientists reported opposite trends (e.g. *Western and Grayson*, 1998; *Famiglietti et al.*, 1998), were unable to detect a trend (e.g. *Hawley et al.*, 1983; *Charpentier and Groffman*, 1992), or found the trend to depend on the mean soil moisture state (e.g. *Owe et al.*, 1982; *Albertson and Montaldo*, 2003). Although many scientists have speculated about the origin of soil moisture variability, only few have tried to quantitatively explain the apparent contradictions in observed soil moisture variability trends by looking at how the different controls interact.

Here we develop a simple model that is able to reproduce observed soil moisture variability trends for the three different data sets studied, and analyse the model results with an extension of the theoretical framework recently developed by *Albertson and Montaldo* (2003) to quantify soil, vegetation, and landscape controls on soil moisture variability. The results might lead to improved understanding of soil moisture variability observations and the aggregation problem.

Data Three datasets are used in this study, each with a different trend of variability with changing mean moisture content (Figure 2.7, upper panels).

Soil moisture (0–20 cm) variability was measured at an agricultural field in Louvain-la-Neuve (Belgium) at 60 days between 30 May 1999 and 13 September 1999 as part of a campaign with the objective to investigate the within-field spatial variability of transpiration (*Hupet and Vanclooster*, 2002). The soils in the field are classified as well-drained silty-loam and there is little topography. During the campaign the field was cropped with maize. The climate is moderate humid. Meteorological observations are available from 1 January 1999 till 31 December 1999.

From 24 June 1998 to 26 Januari 1999, soil moisture (0–30 cm) was measured with 36 TDR sensors (spacing 1 m) at a gently sloping field transect at the Virginia Coastal Reserve Long Term Ecological Research (VCR-LTER) site on the eastern shore of Virginia (*Albertson and Montaldo*, 2003). The soils were classified as sandy loam, with a vegetation of Johnson grass. Meteorological observations are available for the period 30 June 1998 till 27 September 1998.

The Australian Tarrawarra dataset results from an experiment that aimed at investigating the spatial pattern of soil moisture at the small catchment scale. Between 27 September 1995 and 29 November 1996 a total of 13 soil moisture (0–30 cm) patterns were measured (*Western and Grayson*, 1998). Additional measurements are summarized in *Western et al.* (2004). The soils in the catchment are silty-loam to clay, and the landscape is undulating with a maximum relief of 27 m. The climate is temperate. Land use is perennial pastures used for grazing. Meteorological observations are available for the period 10 August 1995 till 25 October 1997.

Modeling soil moisture variability Under most conditions, lateral flow in the upper part of the soil can be neglected, and the vertically integrated soil moisture balance over a depth L can be written as:

$$\frac{\mathrm{d}\theta}{\mathrm{d}t} = \frac{1}{L}(T - R - q - S) \tag{2.1}$$

where θ is the depth-averaged soil moisture content, T the throughfall, R the saturation excess runoff, q is the drainage at depth L, and S the root water uptake. Here, $L = 0.5$ m and $\mathrm{d}t = 1$ d. Throughfall is the rainfall P that is not intercepted by vegetation, and the size of the interception reservoir is taken proportional to LAI. We assume bare soil evaporation to be small in comparison to the root uptake over the entire profile. Drainage is calculated using Darcy's law with the unit-gradient assumption, and applying the $k(\theta)$ parameterization proposed by *Campbell* (1974). The vertically integrated root water uptake S is a function of the root fraction, a soil moisture stress function, LAI (following *Al-Kaisi et al.*, 1989), and potential evapotranspiration. For Louvain-la-Neuve, the positive relation between LAI and S was confirmed by *Hupet and Vanclooster* (2004). LAI is modeled with a spatial and temporal component. The applied model sufficienty captures the non-linearities and dynamics of the soil moisture loss processes, and similar models have proven succesful in reproducing point scale soil moisture dynamics (e.g. *Albertson and Kiely*, 2001; *Laio et al.*, 2001).

We reproduce the first and second order spatial moments of θ ($\bar{\theta}$ and σ_m^2) by running a large ensemble of the model with variable parameters. Initial conditions of θ are set by taking $q = 1$ mm d^{-1}. We assume both the logarithm of the saturated hydraulic conductivity k_s and LAI to follow a normal distribution. Local soil parameters are related to k_s by linear regression with $\ln(k_s)$, fitted to the data provided by *Clapp and Hornberger* (1978). Due to the positive effect of high k_s on canopy growth through better aeration, soil temperature and water transport to roots, we assume $\rho(\ln(k_s), \mathrm{LAI}_{max}) = 1$. Atmospheric forcing was calculated from available observations and assumed to be constant in space.

In order to account for spatial differences in the water balance caused by differences in exposure due to sloping of the landscape, we follow *Svetlitchnyi et al.* (2003) and write the effect of topography on the available moisture content $\theta^* = \theta - \theta_w$ in the top 0.5 m of the soil in terms of a wetness coefficient η:

$$\theta_t^* = \eta \cdot \theta^* \tag{2.2}$$

where θ_t^* is the "corrected" value of θ^*. η depends on slope profile shape, slope aspect, distance from the divide, and slope gradient, and can be derived from a digital elevation model. As a

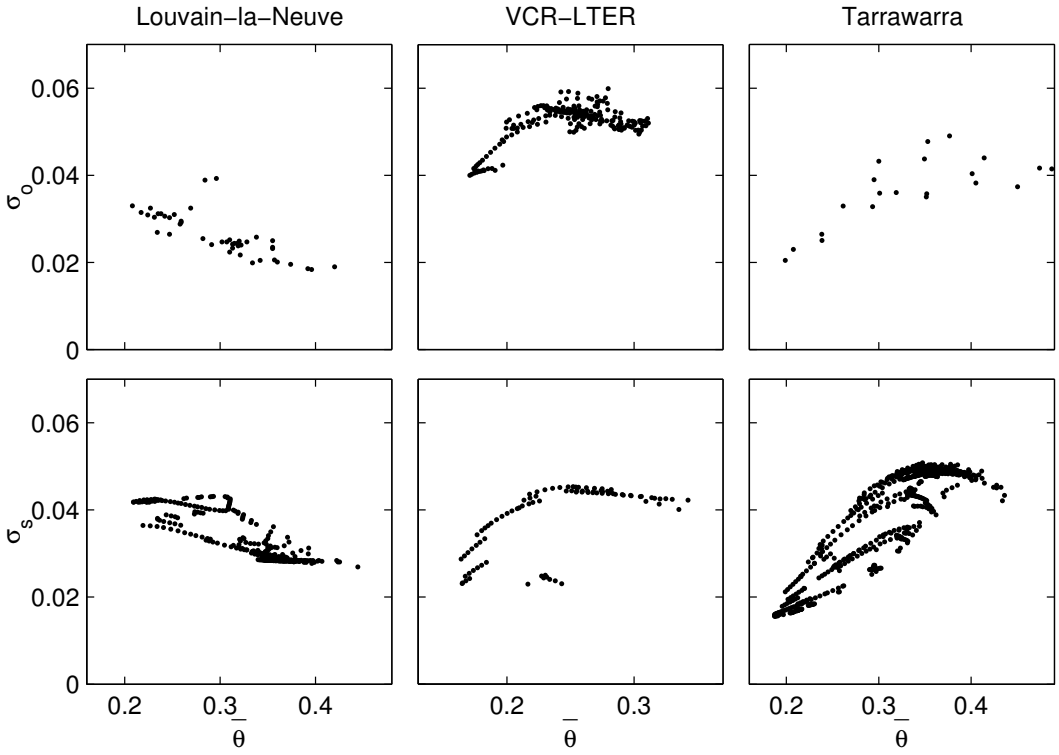

Figure 2.7: Observed (σ_o) and simulated (σ_s) soil moisture standard deviation as function of mean soil moisture content ($\overline{\theta}$).

first order approach, we add the variance caused by (2.2) to σ_m^2, assuming $\overline{\eta} = 1$. To allow direct comparison with observations, we also account for apparent variability due to a measurement error ε ($\overline{\varepsilon} = 0$). The total simulated soil moisture variance σ_s^2 can now be written as:

$$\sigma_s^2 = \sigma_m^2 + \sigma_\eta^2 \cdot \overline{\theta^*}^2 + \varepsilon^2 \tag{2.3}$$

Figure 2.7 shows that both the range of $\overline{\theta}$ as well as the magnitude, trend, and hysteresis effects of σ_s compare well to the observations.

Analysis In order to distinguish the contribution of different controls on the time evolution of σ_s, we first follow *Albertson and Montaldo* (2003). Substracting the spatial average equivalent of (2.1) from (2.1) yields an expression for the time evolution of a local soil moisture anomaly:

$$\frac{\mathrm{d}\theta'}{\mathrm{d}t} = \frac{1}{L}(T' - R' - q' - S') \tag{2.4}$$

where $'$ denotes a deviation from the spatial average. Multiplying (2.4) by $2\theta'$, performing a chain rule operation to the left hand side, and averaging the result yields:

$$\frac{\mathrm{d}\overline{\theta'^2}}{\mathrm{d}t} = \frac{\mathrm{d}\sigma_m^2}{\mathrm{d}t} = \frac{2}{L}\left(\overline{\theta' T'} - \overline{\theta' R'} - \overline{\theta' q'} - \overline{\theta' S'}\right) \tag{2.5}$$

which is an expression for the time evolution of the spatial soil moisture variance. Since the right-hand side of (2.5) consists of covariance terms, their contribution depends on both the magnitude

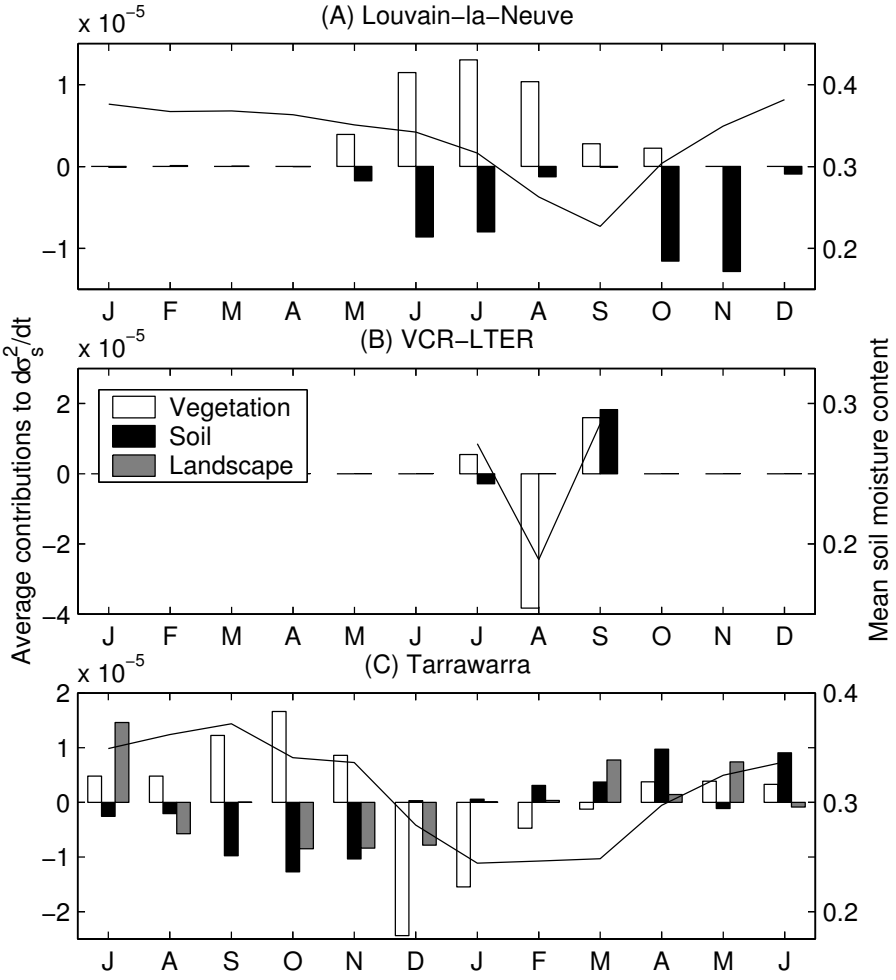

Figure 2.8: Monthly average vegetation, soil, and landscape contributions to $\mathrm{d}\sigma_s^2/\mathrm{d}t$, as in (2.6).

of soil moisture and flux anomalies as well as their mutual correlation. The sign of the correlation controls whether the different processes act to create or destroy spatial soil moisture variance (see *Albertson and Montaldo*, 2003, for synthetic examples). Combining (2.5) with the time derivative of (2.3) yields:

$$\frac{\mathrm{d}\sigma_s^2}{\mathrm{d}t} = \underbrace{\frac{2}{L}\left(\overline{\theta' T'} - \overline{\theta' S'}\right)}_{\text{Vegetation}} \underbrace{-\frac{2}{L}\left(\overline{\theta' R'} + \overline{\theta' q'}\right)}_{\text{Soil}} \underbrace{+\sigma_\eta^2 \frac{\mathrm{d}\overline{\theta^*}^2}{\mathrm{d}t}}_{\text{Landscape}} \tag{2.6}$$

Rather than evaluating all terms seperately, we group the correlated terms as (local) vegetation and soil controls, and non-local landscape control. Figure 2.8 explains the different trends in Figure 2.7 by evaluating the contribution of the different groups in (2.6). For clarity the terms have been converted to monthly averages.

In the Louvain-la-Neuve dataset, soil moisture variability increases during the growing season. During winter and spring (December–April), precipitation surplus causes soil moisture to retain near field capacity, and the variance is fully adjusted to the soil footprint (Figure 2.8A). Untill July, increases in variance due to heterogeneous transpiration are effectively (although not entirely)

cancelled out by drainage. When drainage becomes neglectible (August–September), vegetation controls start to create additional variance. This increase is only destroyed during the first rainfall events in the late growing season (October–November), when the variance is "reset" to the soil footprint ($\overline{\theta' q'} > 0$). It should be noted that also during summer $\theta > \theta_c$ so that root water uptake is under atmospheric control, and ($\overline{\theta' S'} < 0$).

For the VCR-LTER data, this behavior is almost opposite (Figure 2.8B). The coarse soils in combination with high E_p limit root water uptake early during a drying cycle. The (small) initial increase in σ_s during July (Figure 2.7, not visible in monthly average value in Figure 2.8), is due to heterogeneous but unstressed transpiration ($\overline{\theta' S'} < 0$). During the second half of July this changes rapidly, and stressed transpiration causes a sharp decrease in variance ($\overline{\theta' S'} > 0$). Similar to the Louvain-la-Neuve case, rainfall events in September force σ_s to readjust to the soil footprint, only here $\overline{\theta' q'} < 0$.

Tarrawarra shows a more complex pattern (Figure 2.8C). In spring, vegetation controls act to create variance ($\overline{\theta' S'} < 0$), but this variance is initially destroyed by drainage of rainfall. In this period, drying of the soil ($\mathrm{d}\overline{\theta^*}^2/\mathrm{d}t < 0$) causes a transition from non-local to local controls on σ_s (*Grayson et al.*, 1997). This can be seen by the negative landscape contributions. Later during summer (December–February), soil and landscape controls become effectively zero due to advanced drying. The strong soil controlled root water uptake ($\theta < \theta_c$) causes a transition of the sign of the correlation between S and θ ($\overline{\theta' S'} > 0$) resulting in a strong decrease in σ_s^2. The readjustment to the winter soil moisture state is accompanied by an increase in σ_s^2 caused by soil and (non-local) landscape controls.

Discussion Our simulations show that both soil and vegetation controls can act to either create or destroy spatial variance. The main discriminating factor between both behaviors is wether or not the soil dries below θ_c. This depends on the soil texture as well as on the depth of the drying phase. The fact that much of the observed soil moisture variability is actually created by vegetation anomalies (and thus $\rho(\theta, \xi) \neq 0$) calls for new approaches to the soil moisture aggregation problem. This suggests that future field campaigns can further contribute to our understanding of the soil-vegetation-atmosphere system not only by looking at soil moisture variability, but also at how this variability is related to anomalies in soil and vegetation characteristics.

Acknowledgments François Hupet and John Albertson are greatly acknowledged for providing access to their data sets.

Bibliography

Al-Kaisi, M., L. Brun, and J. Enz, Transpiration and evapotranspiration from maize as related to leaf area index, *Agr. Forest Meteorol., 48*, 111–116, 1989.

Albertson, J., and G. Kiely, On the structure of soil moisture time series in the context of land surface models, *J. Hydrol., 243*, 101–119, 2001.

Albertson, J., and N. Montaldo, Temporal dynamics of soil moisture variability: 1. Theoretical basis, *Water Resour. Res., 39*(10), 1274, doi:10.1029/2002WR001616, 2003.

Campbell, G., A simple method for determining unsaturated conductivity from moisture retention data, *Soil Science, 117*(6), 311–314, 1974.

Charpentier, M., and P. Groffman, Soil moisture variability within remote sensing pixels, *J. Geophys. Res., 97*(D17), 18,987–18,995, 1992.

Clapp, R., and G. Hornberger, Empirical equations for some soil hydraulic properties, *Water Resour. Res., 14*(4), 601–604, 1978.

Crow, W., and E. Wood, Impact of soil moisture aggregation on surface energy flux prediction during SGP'97, *Geophys. Res. Lett., 29*(1), doi:10.1029/2001GL013796, 2002.

Famiglietti, J., J. Rudnicki, and M. Rodell, Variability in surface moisture content along a hillslope transect: Rattlesnake Hill, Texas, *J. Hydrol., 210*, 259–281, 1998.

Famiglietti, J., J. Devereaux, C. Laymon, T. Tsegaye, P. Houser, T. Jackson, S. Graham, M. Rodell, and P. Oevelen, Ground-based investigation of soil moisture variability within remote sensing footprints during the Southern Great Plains 1997 (SGP97) Hydrology Experiment, *Water Resour. Res., 35*(6), 1839–1851, 1999.

Grayson, R., A. Western, F. Chiew, and G. Blöschl, Preffered states in spatial soil moisture patterns: Local and nonlocal controls, *Water Resour. Res., 33*(12), 2897–2908, 1997.

Hawley, M., T. Jackson, and R. McCuen, Surface soil moisture variation on small agricultural watersheds, *J. Hydrol., 62*, 179–200, 1983.

Hupet, F., and M. Vanclooster, Intraseasonal dynamics of soil moisture variability within a small agricultural maize cropped field, *J. Hydrol., 261*, 86–101, 2002.

Hupet, F., and M. Vanclooster, Sampling strategies to estimate field areal evapotranspiration fluxes with a soil water balance approach, *J. Hydrol., 292*, 262–280, doi:10.1016/j.jhydrol.2004.01.006, 2004.

Koster, R., M. Suarez, R. Higgins, and H. V. den Dool, Observational evidence that soil moisture variations affect precipitation, *Geophys. Res. Lett., 30*(5), 1241, doi:doi:10.1029/2002GL016571, 2003.

Laio, F., A. Porporato, L. Ridolfi, and I. Rodriguez-Iturbe, Plants in water-controlled ecosystems: active role in hydrologic processes and response to water stress ii. Probabilistic soil moisture dynamics, *Adv. Water Resour., 24*, 707–723, 2001.

Owe, M., E. Jones, and T. Schmugge, Soil moisture variation patterns observed in Hand County, South Dakota, *Water Resour. Bull., 18*(6), 949–954, 1982.

Svetlitchnyi, A., S. Plotnitskiy, and O. Stepovaya, Spatial distribution of soil moisture content within catchments and its modelling on the basis of topographic data, *J. Hydrol.*, *277*, 50–60, 2003.

Western, A., and R. Grayson, The Tarrawarra data set: soil moisture patterns, soil characteristics, and hydrological flux measurements, *Water Resour. Res.*, *34*(10), 2765–2768, 1998.

Western, A., S. Zhou, R. Grayson, T. McMahon, G. Blöschl, and D. Wilson, Spatial correlation of soil moisture in small catchments and its relationship to dominant spatial hydrological processes, *J. Hydrol.*, *286*, 113–134, 2004.